J. Fluid Mech. (1985), *vol.* 156, *pp.* 419–437
Printed in Great Britain

Wall-layer structure and drag reduction

By W. G. TIEDERMAN, T. S. LUCHIK AND D. G. BOGARD†
School of Mechanical Engineering, Purdue University, W. Lafayette, Indiana 47907 USA

(Received 2 July 1984)

When drag-reducing additives are confined entirely to the linear sublayer of a turbulent channel flow of water, both the spanwise spacing and bursting rate of the wall-layer structure are the same as those for a water flow and there is no evidence of drag reduction. Drag reduction is measured downstream of the location where the additives injected into the sublayer begin to mix in significant quantities with the buffer region ($10 < y^+ < 100$)‡ of the channel flow. At streamwise locations where drag reduction does occur and where the injected fluid is not yet uniformly mixed with the channel flow, the dimensionless spanwise streak spacing increases and the average bursting rate decreases. The decrease in bursting rate is larger than the corresponding increase in streak spacing. The wall-layer structure is like the structure in the flow of a homogeneous, uniformly mixed, drag-reducing solution. Thus, the additives have a direct effect on the flow processes in the buffer region and the linear sublayer appears to have a passive role in the interaction of the inner and outer portions of a turbulent wall layer.

1. Introduction

Among the various methods proposed for reducing the viscous drag of turbulent flows, the addition of small amounts of soluble long-chain, high-molecular-weight polymer molecules to liquid flows has been one of the most successful techniques. As clearly demonstrated by Wells & Spangler (1967), Wu & Tulin (1972) and McComb & Rabie (1979), the additive must be in the wall region for drag reduction to occur. When drag reduction occurs in flows of uniformly mixed solutions of polymer additives, the dimensionless transverse spacing of the low-speed streaks within the viscous sublayer increases as reported by Eckelman, Fortuna & Hanratty (1972), Donohue, Tiederman & Reischman (1972), Achia & Thompson (1977) and Oldaker & Tiederman (1977). Since polymer additives both lower the wall shear stress and modify the wall-layer structure, experiments designed to identify the features of the turbulent flow that are directly affected by the polymer additive can provide new knowledge about the physics of both drag reduction and Newtonian 'wall' turbulence.

One objective of the present study was to determine if the presence of a drag-reducing polymer solution in only the viscous sublayer of a turbulent channel flow of water would yield drag reduction and/or modify either the spatial structure of the low-speed sublayer streaks or the bursting rate of these streaks.§ A key question was, does the linear sublayer have an active or a passive role in the drag-reduction process?

† Presently at University of Texas-Austin.

‡ The superscript + denotes a dimensionless quantity scaled with the kinematic viscosity ν and the wall shear velocity $v^* = (\tau_w/\rho)^{\frac{1}{2}}$.

§ These experiments were conducted prior to the publication of McComb & Rabie's (1982) results which answered the drag reduction portion of this objective.

This objective was motivated by previous experiments which have shown an increased spacing of sublayer streaks for drag-reducing flows. This increased spacing led Donohue *et al.* (1972) to hypothesize that the ability of the polymer solution to resist vortex stretching could inhibit the formation of wall-layer streaks. The smaller number of streaks would yield a decrease in the spatially averaged bursting rate which in turn would yield a decrease in turbulent transport and lower viscous drag. This explanation of how the polymer affects the turbulence was adopted because Donohue *et al.* (1972), Achia & Thompson (1977) and Tiederman, Smith & Oldaker (1977) all reported that the time between bursts of a streak were the same for a flow of water and for a drag-reducing flow of a polymer solution at the same wall shear stress. It was also shown by Oldaker & Tiederman (1977) that at the higher values of drag reduction (above 35–40 %), the dimensionless streak spacing increases as the distance from the wall decreases from $y^+ \approx 2$. This increase may indicate stronger damping by the polymer solutions very near the wall. Motion pictures from that study also indicated increased damping of transverse streak movement.

There is considerable evidence, as reviewed by Willmarth (1975) and Cantwell (1981), that the production of turbulent kinetic energy in a wall flow occurs in a coherent quasi-periodic fashion. This process consists of the penetration of high-momentum fluid into the near-wall region and the subsequent ejection of low-momentum fluid from the near-wall region. These three-dimensional sweeps of high-momentum fluid toward the wall and ejections of low-momentum fluid from the wall are separated in both space and time by relatively quiescent periods where little turbulent transport occurs. Essentially, all of the turbulent kinetic energy is produced and most of the turbulent transport occurs during these sweep and ejection events. Since this is a cyclic process in a homogeneous, fully developed flow, it is only necessary for the polymer solution to inhibit one of the events in the cycle to produce an effect on the collective behaviour of the cycle. Therefore, the observation of an increased spacing in a fully developed flow of a homogeneous solution does not preclude the possibility that some other feature of the cycle is directly affected by the polymer. In other words, the increased spacing of the low-speed streaks may be simply the observed 'symptom' and not the 'direct effect' of the polymer molecules.

The other most logical process within the wall region where the polymer could directly affect the turbulent-production cycle is the ejection or bursting process that occurs in the buffer region. This is the region into which the low-speed streaks migrate by lifting away from the wall and where they undergo a high-frequency oscillation before breaking up and ejecting fluid away from the wall (see Kline *et al.* 1967; Kim, Kline & Reynolds 1971). This ejection event begins at a dimensionless distance from the wall in the range $10 < y^+ < 30$.

Virk (1975) proposed that the polymer inhibits the breakup and ejection of fluid from low-speed streaks and this was the original hypothesis that motivated the studies conducted by Donohue. Lumley (1977) also hypothesized that the polymer must have its effect in the buffer region of the flow. Consequently, prior to the present experiments there were two hypotheses about how the polymer acts to reduce drag. One assumed that the polymer acts in a region $y^+ < 4$ to inhibit the formation of low-speed streaks. The other assumed that the polymer acts in a region $10 < y^+ < 30$ to inhibit the breakup of low-speed streaks and the subsequent ejection of low-momentum fluid.

The initial phase of the present experimental programme was designed to test whether or not the polymer additives can be effective when they are only in the linear sublayer. This was accomplished by determining both the spatial structure of the

sublayer and the drag reduction immediately downstream of the injection of a drag-reducing polymer solution into a fully developed channel flow of water. The injection was controlled so that the polymer remained within the viscous sublayer for some distance. Hence, immediately downstream of the slot, the only mechanism by which the polymer could affect the flow structure was by inhibiting the formation of low-speed streaks. Both streak-spacing and drag-reduction measurements were made before the polymer had diffused far enough from the wall to affect the breakup and ejection part of the cycle.

The second objective was to determine how the bursting rate of the wall-layer structure was affected by the presence of drag-reducing solutions within various portions of the wall region. Experiments were conducted in which two different portions of the wall region contained the drag-reducing solution.

In the first case, the measurements were made with dyed fluid injected through a thin slot with an injection flow rate equal to one-tenth the undisturbed flow rate in the linear sublayer. Using this technique, the visually detected bursts represented the initial convective transport from a sublayer containing the drag-reducing solution.

In the second case two sets of slots were used. Drag-reducing solutions were injected at a rate equal to the flow rate in the linear sublayer through the upstream slot while the downstream slots were used to mark sublayer fluid. In this way bursts were detected in a region where the drag reduction from the fluid entering the channel through the upstream slot was near a maximum and the injected solution had mixed with at least the buffer region of the original water flow.

The present experiments differed in one fundamental way from previous experiments designed to determine bursting rates in homogeneous flows of drag-reducing solutions. The experiments by Donohue *et al.* (1972) and Achia & Thompson (1977), which yielded bursting data for drag-reducing flows, used flow-visualization methods introduced by Kline *et al.* (1967). The procedure for the Kline method is to count *all* bursts marked by fluid seeped into the wall region from a short spanwise slot. In order to observe all of the marked bursts, a rather long streamwise field of view is required. For example, in a water flow the bursts will originate from $100 < x^+ < 1500$ downstream of the slot. This occurs because the marked fluid must be swept into a streak and the streak must lift or migrate away from the wall before it will eject marked wall-region fluid into the outer portion of the flow. Similarly at a downstream location where the dyed fluid is exhausted, no new bursts can be detected even though bursts are occurring. In both of the earlier drag-reduction studies cited above, the streamwise field of view was of the order of $x^+ = 1000$–2000. This was an adequate field of view for the water cases. However, as shown by Tiederman *et al.* (1977), this streamwise view probably was not sufficient for drag-reducing flows where the sublayer streaks are much longer.

Consequently, a second method for determining the average time between bursts from dye-slot flow visualization was introduced by Tiederman *et al.* (1977). This new method was based on the concept that, even though the bursting rate of marked fluid increases from zero and then eventually decreases with streamwise distance, the actual bursting rate cannot be a function of streamwise distance in a fully developed flow. Hence, if there is a streamwise region where dyed fluid seeped through a wall slot marks all of the bursts, then that region will be defined by a plateau in a plot of the number of ejections per unit time as a function of distance from the dye slot. The plausibility of this method was demonstrated by Tiederman *et al.* (1977) and later developed and proven by Bogard & Tiederman *et al.* (1983) using one-to-one

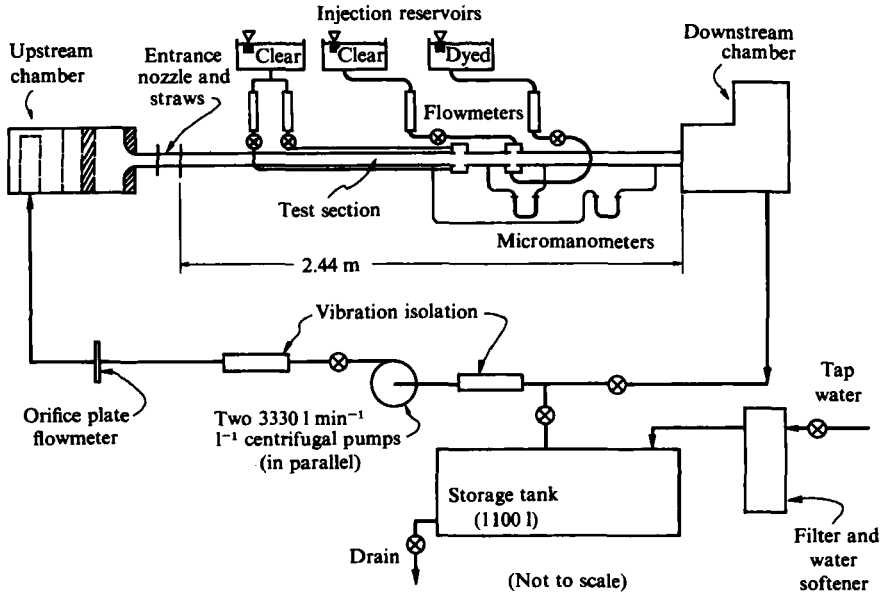

FIGURE 1. Schematic of flow loop.

comparisons between dye-marked ejections and those marked by a hydrogen-bubble wire oriented normal to the surface. This new technique is more accurate and it was used for all the bursting-rate results in this paper.

Since the injection-slot width was the main experimental variable which allowed the polymer solution either to seep into the sublayer or to be injected into the buffer region, the results are organized by injection slot. The thin slots had a width of 0.130 mm and were used to seep solutions and/or dyed fluid into the sublayer at a rate equal to one-tenth the sublayer flow rate. Inclined slots with a streamwise gap of 1.30 mm were used to inject solutions at a rate equal to the sublayer flow rate.

2. Experimental apparatus and procedures

2.1. *Apparatus*

The experiments were conducted in the flow loop shown in figure 1. Water was circulated by centrifugal pumps whose flow rate was measured by a sharp-edged orifice. Fluid entered the upstream stilling chamber through a 10 cm-diameter plastic pipe which extended from the bottom of the chamber to near the top. This pipe was capped at the top and uniformly perforated with 13 mm holes that initially distributed the incoming flow. A perforated plate and a screen–sponge–screen section separated the inlet of the upstream chamber from its outlet. The outlet was a smooth two-dimensional contraction from the 60×60 cm cross-section of the upstream chamber to the 2.5×25 cm cross-section of the channel. Immediately downstream of this contraction was a flow straightener made of closely packed plastic drinking straws, 197 mm long and 5.6 mm i.d. Consequently the flow entered the test section without any large-scale vorticity.

At the downstream end of the test section, a large stilling tank ensured that disturbances from the outlet were not transmitted upstream. Located in this

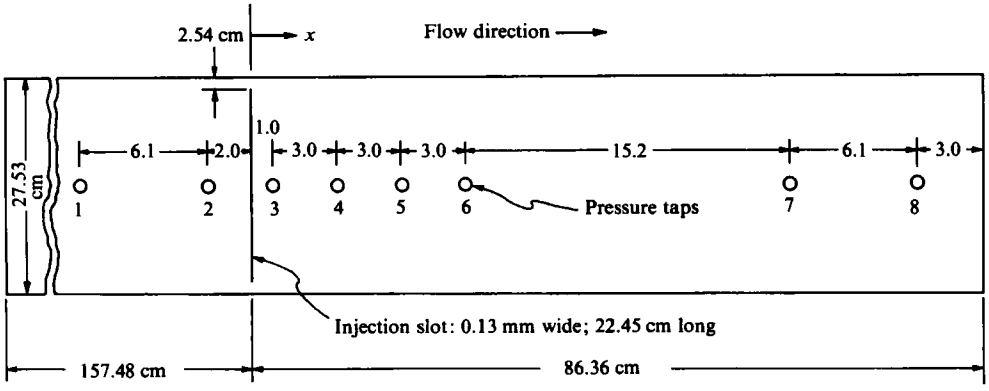

(Distances between pressure taps measured in channel heights) (Not to scale)

FIGURE 2. Bottom wall of channel with a single slot.

downstream tank was a cooling coil for temperature control. The two stilling tanks as well as the test section were constructed from 13 mm clear acrylic sheets.

The internal dimensions of the rectangular cross-section of the channel were 2.5×25 cm which gave the channel an aspect ratio of 10 to 1. The injection slots were located more than 60 channel heights downstream of the channel entrance and more than 30 channel heights upstream of the exit. Consequently the flow in the region of the injection slots was typical of fully developed, two-dimensional channel flow.

The injected fluid flowed by gravity from reservoirs above the channel, through rotameters and flow-control valves to the injection slots. As shown in figure 1, a separate system supplied fluid to slots in each of the 25 cm walls of the channel. Clear fluid was supplied to the slots in the top wall while dyed fluid was piped to the downstream bottom slot. The rotameters were calibrated for each injected fluid.

A schematic of the bottom wall with only a 0.130 mm width injection slot in place is shown in figure 2. Notice that the slot was 22.5 cm long and that it was centred in the 27.54 cm plate that formed one of the 25 cm walls of the test section. As a result, fluid was not injected into either the corners or along the 2.5 cm sidewalls of the channel.

Also shown in figure 2 are the streamwise locations of the pressure taps that were centred in the bottom wall of the channel. Tap number 1 was 8 channel heights upstream of the injection slots and tap number 8 was 31 channel heights downstream of the slots.

The bottom plate of the modified test section is shown in figure 3. The major addition is injection slot 1 which had a streamwise gap of 1.30 mm and introduced fluid at an angle of 25° with respect to the wall. Injection slot 2 was the original slot in this wall and it was used only for flow-visualization purposes while the larger upstream slot was used for introducing the injected solutions. Note that the distribution of pressure taps around the slots differed from the configuration for the original bottom plate.

For both test sections the top plate had identical injection slots at the same location as the bottom plate. There were no pressure taps in the top plates.

Two micrometer manometers with carbon tetrachloride as the manometer fluid were used to measure the pressure drop. With this manometer fluid the pressure measurements could be made with a sensitivity of $\pm 1.5 \times 10^{-2}$ mm of water.

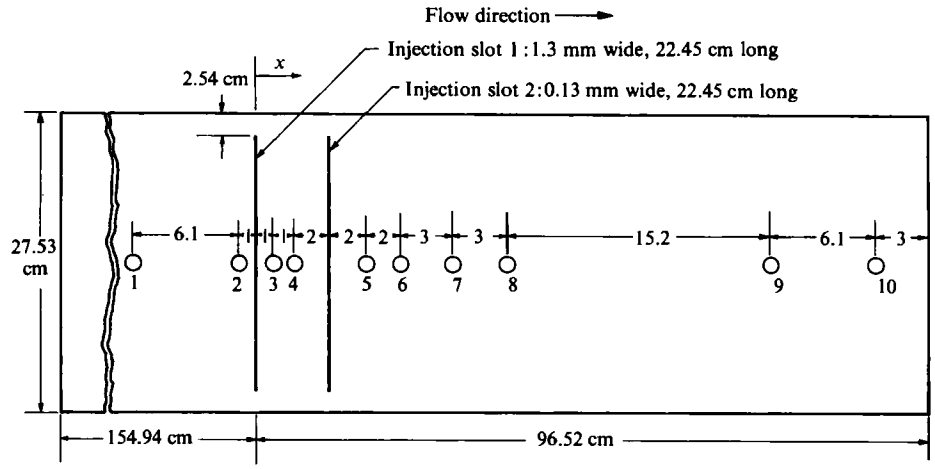

FIGURE 3. Bottom wall with two slots.

Video records of ejections and sublayer streaks were made with a Video Logic Corporation INSTAR IV high-speed motion analyser. The system has simultaneous two-camera capability and utilizes a synchronous strobe which gives each camera an effective exposure time of 10 μs. The cameras produce 120 frames per second that are recorded on 1 inch video tape. The tape may be played back at the recording speed and in various slow-motion formats including frame-by-frame.

The fluorescent fluid was a 2 or 4 g l^{-1} concentration of fluorescein disodium salt. The fluids injected into the water flows were water, a 100 p.p.m. solution of SEPARAN AP-273, a 200 p.p.m. solution of AP-273, a 400 p.p.m. solution of AP-273, and two mixtures of glycerin and water which matched the viscosity of the 100 p.p.m. and 400 p.p.m. polymer solutions. Viscosities of all injected fluids, both clear and dyed, were measured with a LVT-SCP Wells–Brookfield, 1.565° cone and plate, microviscometer at shear rates of 115 and 230 s^{-1}. The dye did not affect the viscosity of the injected fluids.

The drag-reducing capability of both dyed and clear polymer solutions used in the channel were verified by measurements in a separate, horizontal 14.05 mm i.d. tube. The tube was gravity fed from an upstream reservoir while the flow rate was measured by timing the collection of a fixed mass of fluid. The pressure drop from two taps separated by 2.00 m was measured with an inverted U-tube, water manometer. The upstream pressure tap was 50.8 cm from the entrance of the tube and the downstream tap was 25.4 cm upstream of the exit. It is important to note that the dye did not affect the drag-reducing capability of the polymer solutions. In addition, the drag-reduction results from different batches of polymer solutions were very similar. The reproducibility of the polymer solutions from batch to batch resulted from consistent mixing procedures.

2.2. *Procedures*

Tap water for the main channel flow passed through a filter and a water softener prior to entering the flow loop. It was de-aerated by heating to about 40 °C and then cooled to room temperature before being circulated in the flow loop.

The polymer solutions and glycerin mixtures were made with filtered tap water.

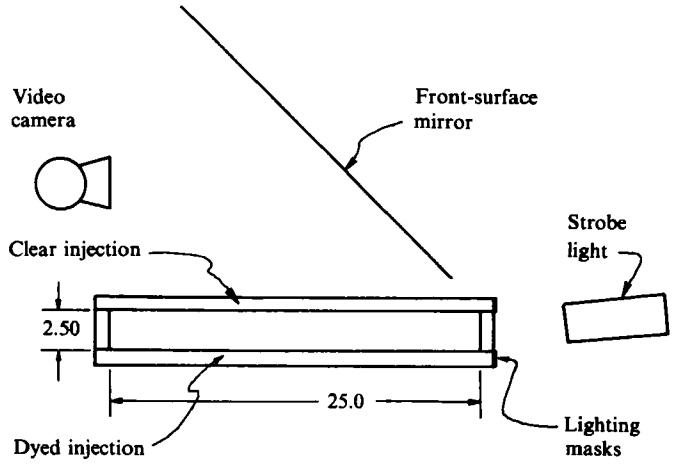

(All dimensions in cm; not to scale)

FIGURE 4. Lighting and camera arrangement for streak-spacing experiments.

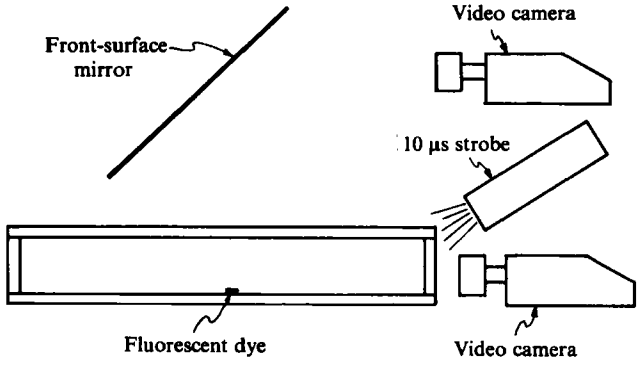

FIGURE 5. Lighting and camera arrangement for ejection-rate experiments with short dye slot.

The water used for the polymer solutions was boiled and then cooled prior to adding the polymer. The polymer solutions initially were mixed to produce concentrations of 800–2560 p.p.m. These concentrated mixtures were allowed to hydrate for 12–24 h prior to dilution to 100, 200 or 400 p.p.m. The quantity of polymer solution prepared in each batch was sufficient to conduct both the drag-reduction confirmation tests in the 14.05 mm tube and the channel-injection experiments.

The lighting and camera configuration used to obtain information about the spatial structure of the sublayer streaks is shown in figure 4. The camera recorded a plan view of the fluorescent, dye-marked streaks on the bottom wall. The line of sight was through the clear fluid injected through the top wall. The data was reduced visually using multiple-observer procedures described by Oldaker & Tiederman (1977).

Two slightly different flow-visualization schemes were used to obtain bursting-rate data. In both cases the objective was to deduce the average bursting rate per unit area from the ejection rate measured in the streamwise region where the dye marks all of the ejection events. Ejections are the rapid motion of fluid away from the wall which comprise the final part of the bursting event described by Kim *et al.* (1971).

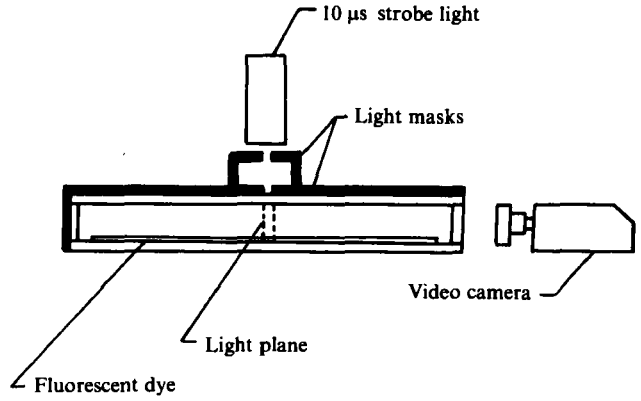

FIGURE 6. Lighting and camera arrangement for ejection-rate experiments with long dye slot.

Offen & Kline (1975) made the initial distinction that one burst could contain more than one ejection. In the present study, an ejection was counted when a dye-marked fluid element originating from a region of $y^+ \leqslant 15$ moved outward from the wall by at least $\Delta y^+ = 20$ in a streamwise distance of $\Delta x^+ = 350$. For the short transverse dye-slot length shown in figure 5, the transverse width of the ejection area was assumed to be $\bar{n}\bar{\lambda}$, where $\bar{n}$ is the average number of streaks marked by the slot and $\bar{\lambda}$ is the average transverse spacing of the streaks. In fact the dye-slot length was selected such that $\bar{n}$, deduced using the analysis of Bogard & Tiederman (1983), yielded $\bar{n} = 1$.

The camera and lighting configuration for the long dye-slot, slit-lighting technique for measuring ejection rates is shown in figure 6. In this technique the transverse width is given by the width of the light slit d_1. As verified by Luchik & Tiederman (1984), the long- and short-dye-slot techniques correspond when one makes the logical assumption that

$$\bar{n} = d_1/\bar{\lambda}.$$

Physically a burst contains one or more ejections that arise from a single instability of one streak. For flows of water, Offen & Kline (1975) and Bogard & Tiederman (1983) showed that on average there are two ejections of dyed fluid per burst. Consequently, for a water flow the average bursting rate is $\frac{1}{2}$ the average ejection rate. The lighting and camera arrangement shown in figure 5 was used in the present study to determine the average number of ejections per burst for flows with drag reduction.

The amount of drag decrease or increase was deduced from measurements of the pressure using the wall taps in the bottom plate of the channel (see figures 2 and 3). For fully developed flow with no injection the pressure gradient is proportional to the wall shear stress, and thus the viscous drag. With fluid injection, the assumption that the flow is fully developed is not strictly correct in the vicinity of the slot. This issue will be discussed further when the drag-reduction results are presented. The other consideration with our injection is that, by design, the slots did not place any drag-reducing solution in the endwall areas. Since these endwall areas are regions of relatively lower shear stress, we have chosen to make a two-dimensional assumption and simply calculate the percentage drag reduction over the region between two wall taps as

$$\% \text{ DR} = \frac{\Delta P - (\Delta P)_{\text{i}}}{\Delta P} \times 100.$$

Experiment number	Injected fluid	C_i	Q_i (ml/min)	Re_h	$\nu \times 10^6$ (m^2/s)	$\nu_i \times 10^6$ (m^2/s)	Spacing (S) or bursting (B) measurements	Figure describing lighting configuration
			experiments with 0.130 mm slot					
1	water	0	40	17600	0.916	0.916	S	4
2	glycerin	16%	40	17600	0.916	1.38	S	4
3	AP-273	100 p.p.m.	40	18100	0.893	1.36	S	4
4	AP-273	100 p.p.m.	40	17400	0.926	1.28	pressure drop only	
5	glycerin	36%	40	17400	0.928	2.90	S	4
6	AP-273	400 p.p.m.	40	17800	0.905	2.75	S	4
7	water	0	40	17800	0.907	0.907	B	6
8	glycerin	16%	40	17800	0.907	1.35	B	6
9	AP-273	100 p.p.m.	40	17800	0.907	1.32	B	6
10	glycerin	36%	40	17800	0.907	2.71	B	6
11	AP-273	400 p.p.m.	40	17800	0.907	2.34	B	6
			experiments with 1.30 mm slot					
12–16	water	0	0	17800	0.907	—	B	6
17	water	0	400	17800	0.907	0.907	S&B	4&6
18	water	0	0	17800	0.907	—	B	6
19	water	0	0	15000	0.907	—	S&B	4&6
20	water	0	0	15000	0.907	—	B	6
21	water	0	0	11000	0.907	—	B	6
22	water	0	0	11000	0.907	—	S&B	4
23	AP-273	100 p.p.m.	400	17800	0.907	1.11	S&B	4&6
24	AP-273	200 p.p.m.	200	17800	0.907	1.16	S&B	4&6
25	AP-273	200 p.p.m.	400	17800	0.907	1.16	S&B	4&6
26	AP-273	100 p.p.m.	400	22300	0.907	0.963	B	5
27	glycerin	16%	400	17800	0.907	1.28	B	6

TABLE 1. Experimental conditions

Here ΔP is the pressure drop between the taps with no injection and $(\Delta P)_i$ is the pressure drop with injection of fluid through the slots.

A summary of the experimental conditions is given in table 1. For the bulk of the experiments the volumetric flow rate of water in the channel was set at 4.51 l s^{-1} which yielded a Reynolds number based on channel height and the average velocity of 17800. For the 0.130 mm slot experiments, the injection rate was 40 ml min^{-1}. This injection rate corresponds to one-tenth of the flow rate between $0 < y^+ < 8$ passing the transverse extent of the slot. This is essentially one-tenth of the flow rate in the undisturbed linear sublayer over each slot. For this and lower flow rates, the injected fluid turned immediately it left the slot and flowed along the wall. The injection rate through the inclined 1.30 mm slots was 400 ml min^{-1}.

3. Results

3.1. *Results for injection through only the* 0.130 *mm slot*

As expected, the pressure differences in the immediate vicinity of the injection slots were those that were affected most by the injection of a fluid. The results shown in table 2 for the injection of water are typical of the results for the injection of

Pressure taps	Distance between taps $\Delta x/h$	Average distance from slot x/h	% DR
2–3	3.05	−0.50	−2
3–4	3.05	2.54	0

TABLE 2. Pressure-drop results for water injection, experiment number 1. DR = drag reduction.

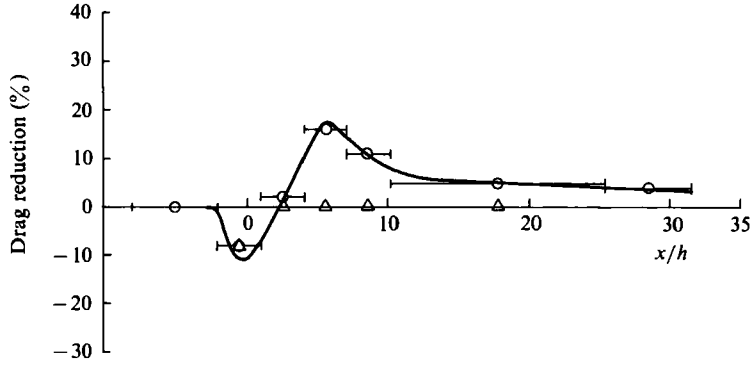

FIGURE 7. Drag reduction as a function of streamwise distance for injection through 0.130 mm slot: ○, 100 p.p.m. AP-273; △, 16% glycerin.

Newtonian fluids. The dimensionless distances shown in the table are normalized with the channel height h. For experiments with the narrow slot the flow rate was set by matching the nominal value of $\Delta P/\Delta x$ in the channel. Positive values of the average streamwise location are downstream of the slot at $x/h = 0$. The small negative drag reduction between pressure tap 2 and tap 3 corresponds to the smallest difference in manometer deflection that can be measured. For $x/h > 1.0$ there is no measurable influence due to the injected water.

The pressure-drop profiles for the injection of a 100 p.p.m. solution of AP-273 and a 16% glycerin solution appear in figure 7. This glycerin solution had essentially the same viscosity as the 100 p.p.m. polymer solution. Figure 8 shows a comparison between the pressure-drop measurements for the 400 p.p.m. AP-273 injection and the 36% glycerin injection which matches the viscosity of the 400 p.p.m. solution. In all four data sets the basis for calculating the amount of drag reduction was the pressure drop with no injection. Recall that there is effectively no difference in the pressure drop between the cases with no injection and with water injection.

Obviously there is a continuous variation of skin friction in the channel flows. However, since the pressure taps are separated by 7.6 cm or more, the data only yield the average pressure drop over the distance between the taps. Consequently, in the drag-reduction figures the data points are plotted at the mid point between pressure taps, and the distance between the pressure taps is shown by a horizontal line with short vertical bars at its ends. The position of the continuous lines drawn through the data was then estimated such that the area bounded by the continuous curve and the x-axis is the same as the area under the horizontal line through the data point and the x-axis. This procedure for estimating the continuous variation of skin friction

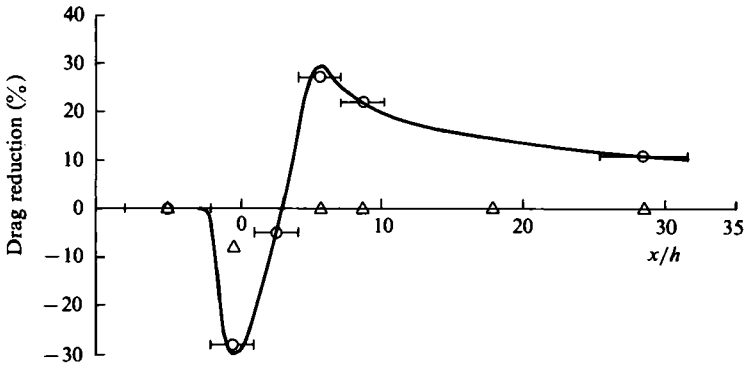

FIGURE 8. Drag reduction as a function of streamwise distance for injection through 0.130 mm slot: ○, 400 p.p.m. AP-273; △, 36% glycerin.

works well with the possible exception of the region very near the slot. The continuous curves indicate that increases in drag occurred upstream of the slot. The data only show that increases in drag occurred in the distance between the two taps (one upstream and one downstream of the injection slot).

There are several points to discuss concerning the results shown in figures 7 and 8. For all cases where either a polymer or a glycerin solution was injected, there is a significant drag increase in the immediate vicinity of the slot. Recall that the injection flow rates are the same as for the water injection where the drag increase is barely detected. This drag increase for the 100 p.p.m. solution has the same peak magnitude as the increase for the 16% glycerin injection. However, the drag increase for the 400 p.p.m. polymer solution is significantly greater in both magnitude and streamwise extent than the increase for the 36% glycerin solution. As will be seen from the flow-visualization results, the polymer solutions do not mix as well with the water flowing in the channel as the glycerin solutions. The degree of mixing also decreases as the concentration of the polymer solution increases. Hence there are potentially two factors which yield these drag increases very near the slot. One is that the viscosity of these glycerin and polymer solutions is higher than that of water. The second is that an unmixed fluid layer along the wall will accelerate the mainstream water flow and produce an increased pressure drop. Assuming that the velocity profile in an injected and unmixed polymer solution flowing along the top and bottom walls is linear, the magnitude of this pressure-drop increase can be estimated using conservation of mass and Bernoulli's equation. Such estimates show that the decrease in mixing alone is sufficient to explain the higher drag increases of the polymer solutions.

Of course neither glycerin solution showed any evidence of drag reduction. Moreover, as for the case of water injection, the injection of these glycerin solutions does not affect the pressure drop for $x \geqslant 2.5$ cm.

A best estimate for the location where drag reduction begins for the 100 p.p.m. solution of AP-273 is $x = 5.1$ cm. This corresponds to $x/h = 2.0$. For the 400 p.p.m. solution, drag reduction appears to begin at $x = 7.6$ cm or $x/h = 3.0$.

The spanwise spacing between streaks was determined by counting the number of streaks in about fifteen statistically independent frames of the video tape and then calculating the average spanwise spacing $\overline{\lambda}$, from

$$\overline{\lambda} = b/\overline{N}.$$

Experiment	Injected fluid	Measurement location x/h	% DR at measurement location	Dimensionless spacing λ^+
1	Water	0.510	−2.3	105
1	Water	0.305	−2.3	107
3	100 p.p.m. AP-273	0.523	−8.0	106
2	16% glycerin	0.510	−2.0	101
2	16% glycerin	0.305	−4.0	101
6	400 p.p.m. AP-273	0.516	−24.0	99
5	36% glycerin	0.504	−1.0	101

TABLE 3. Streak-spacing results downstream of 0.130 mm slots

Here b is the transverse distance in which streaks are counted; $\overline{N}$ is the average number of streaks per frame.

A streak was defined as a clearly identifiable single longitudinal structure with a streamwise length of at least four times the apparent average spanwise spacing between streaks. Streaks were counted at downstream locations identified by a line on an overlay for the video screen.

Four observers counted streaks for each of the results given in table 3. Each observer individually viewed the video tapes at a speed of 3% of the recording speed. The tape was stopped at approximately equal time intervals and streaks were counted. The average number of streaks per frame was calculated for each observer and the mean of these averages was used to determine $\overline{N}$ and $\overline{\lambda}$. The dimensionless streamwise location of these counts as well as the dimensionless spacing $\lambda^+ = \overline{\lambda} v^*/\nu$ and the estimated drag reduction at the measurement location are shown in table 3.

The obvious result clearly shown in table 3 is that the streak spacing when non-dimensionalized with the viscosity of water was the same for all injected fluids. The value of $\lambda^+ \approx 100$ is the value reported for a large number of Newtonian flows (see Smith & Metzner 1983).

While single values are reported for the location of the streak-spacing measurements, it was clear from the pictures that the streak-spacing results apply over a streamwise distance that is close to the average streak length of $x/h = 0.4$ ($x^+ \approx 400$) for water and glycerin injection, and $x/h > 0.4$ for the polymer solutions. This point is made because the drag-reduction curves for the polymer solution vary rapidly in the region of these measurements and hence the single values of drag reduction shown in the table are presented to indicate that no positive drag reduction was measured in the vicinity of these streak-spacing measurements.

In the plan view of the streaks it is possible to make rough estimates of the average location where the streaks begin to mix significantly with fluid further from the wall. For the two experiments where the injected fluid was either water or a glycerin solution, this distance l was 2.5 cm or less ($l/h \leqslant 1.0$). When 100 p.p.m. of AP-273 was injected, there seemed to be slightly less mixing and l was about 2.5 cm. However, for the 400 p.p.m. injection, l was 7.5 cm or more, $l/h \approx 3.0$, with considerably less mixing observed between the sublayer and the rest of the flow. It should be noted that positive drag reduction was not measured for either polymer solution at downstream locations where $x < l$.

Figure 9 shows histograms of the number of ejections counted for the water, 16% glycerin and the 100 p.p.m. AP-273 polymer solution as a function of non-dimensional

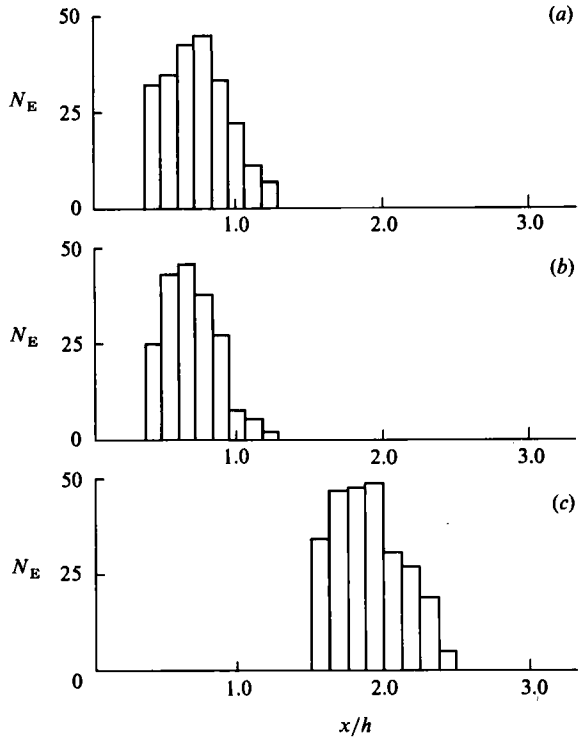

FIGURE 9. Ejection histograms from 4.17 s of data for 0.130 mm slot: (*a*) water; (*b*) 16% glycerin; (*c*) 100 p.p.m. AP-273.

streamwise distance from the 0.130 mm slot. These histograms are typical in that the number of ejections is low near the slot, increases and then decreases again farther downstream. Recall that the marked fluid must be swept into a streak and that the streaks must lift away from the wall before they will burst or eject marked fluid. Thus, some distance is required before all streaks which burst in a given region are marked. Of course, when the marked fluid is depleted far downstream, streak bursting in that region will not be visualized.

The histograms for the water and 16% glycerin injections are nearly the same. The peak values in the distributions as well as the locations of the distributions are very similar. Notice that the histogram for the 100 p.p.m. solution also has the same peak value but it is displaced downstream. This indicates that the polymer solution diffuses at a slower rate from $y^+ \leqslant 2$ to $y^+ \approx 10$–15 than the Newtonian fluids and yet there is no effect on the initial bursting rate at $y^+ = 15$. Since there was negligible drag reduction at $x/h = 2.0$, the fact that the bursting rate does not change at this location is consistent with the view that most of the turbulent transport occurs during bursts.

Similar results, shown in figure 10, were found for the water, 36% glycerin and 400 p.p.m. polymer solutions. As expected the 400 p.p.m. solution diffused even more slowly into the main flow than the 100 p.p.m. polymer solution, moving the region where all ejections are detected further downstream. Ejection-rate results from these experiments are summarized in table 4. Since the peak values of the ejection histograms are the same, the initial bursting rates are the same.

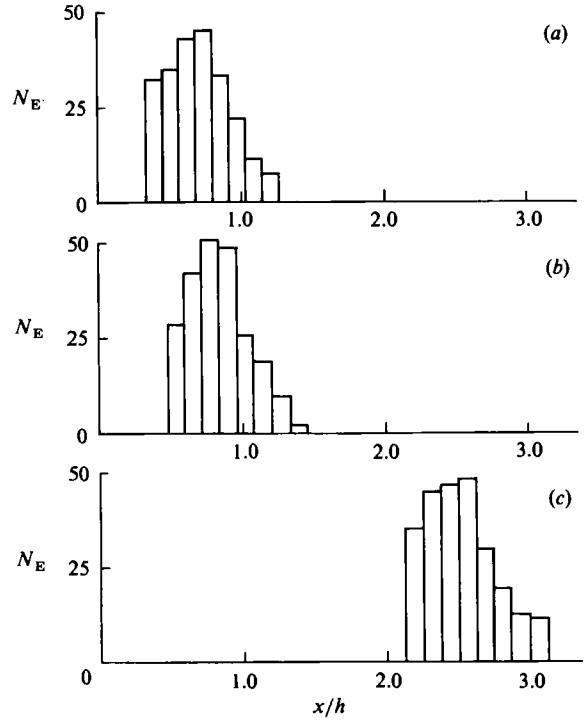

FIGURE 10. Ejection histograms from 4.17 s of data for 0.13 mm slot: (*a*) water; (*b*) 36% glycerin; (*c*) 400 p.p.m. AP-273.

Experiment number	Injection fluid	Average ejection rate per unit area $(m^2\ s)^{-2} \times 10^3$	Average value of x/h in the detection region	% DR in the detection region
7	Water	696	0.736	−1.5
8	16% glycerin	712	0.660	−2.2
9	AP-273 100 p.p.m.	760	1.829	1.0
10	36% glycerin	776	0.864	−2.6
11	AP-273 400 p.p.m.	733	2.540	−2.8

TABLE 4. Bursting-rate results downstream of 0.130 mm slots

3.2. *Results for injection through the* 1.30 *mm inclined slots*

A comparison of the drag reduction which occurred for the 400 ml min^{-1} injection of water, 16% glycerin solution, and 100 p.p.m. solution of AP-273 is shown in figure 11. As expected the water injection had little effect on the pressure distribution except in the immediate vicinity of the inclined injection slot. The influence of the injection of the glycerin extended further downstream; however, it also had a relatively small effect for $x/h \geqslant 10$.

When the 100 p.p.m. SEPARAN AP-273 polymer solution was introduced through the injection slots, there was a noticeable effect on the pressure field in the channel. The maximum drag reduction of approximately 22% was achieved at $x/h = 10$ and

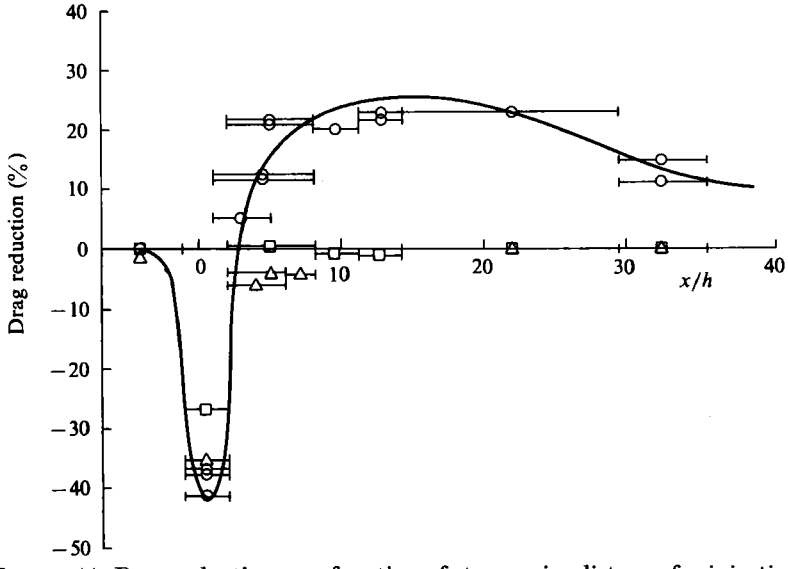

FIGURE 11. Drag reduction as a function of streamwise distance for injection through 1.30 mm slot: □, water; △, 16% glycerin; ○, 100 p.p.m. AP-273.

Experiment number	Fluid injected through inclined slots	Measurement location x/h	% DR at measurement location	Dimensionless spacing λ^+
17	water	0.610	0	97
19	none	0.644	0	88
22	none	0.490	0	108
23	100 p.p.m. AP-273	2.134	22	124
24	200 p.p.m. AP-273	3.556	25	150
25	200 p.p.m. AP-273	3.556	27	147

TABLE 5. Streak-spacing measurements downstream of 1.30 mm, inclined slots

maintained for a streamwise distance of $\Delta x/h = 15$. One should note that, although the drag reduction occurred for a desirable distance, the maximum value is still less than one half that reported by Oldaker & Tiederman (1977) for the flow of a completely mixed solution of 100 p.p.m. AP-273. The onset of positive drag reduction occurs at $x/h = 3.0$ which is essentially the same location as where drag reduction began with the lower injection rate through the smaller slots.

The streak-spacing results obtained downstream of the inclined slots are shown in table 5. The streak spacing has been normalized with the local shear velocity and an estimate of the polymer viscosity at the shear rate in the channel. In all of these experiments two sets of slots were used. The conditions for the injection through the inclined, 1.30 mm slots are given in table 1. The smaller downstream slots were used only for flow-visualization purposes. As a result the flow rate through the downstream slots was 40 ml min^{-1} which is nominally one-tenth the flow rate in the linear sublayer. As shown in the previous sub-section, at these injection rates, the type of fluid injected has no effect on either the streak spacing or the bursting rate. Hence clear and dyed water were used in the flow-visualization slots.

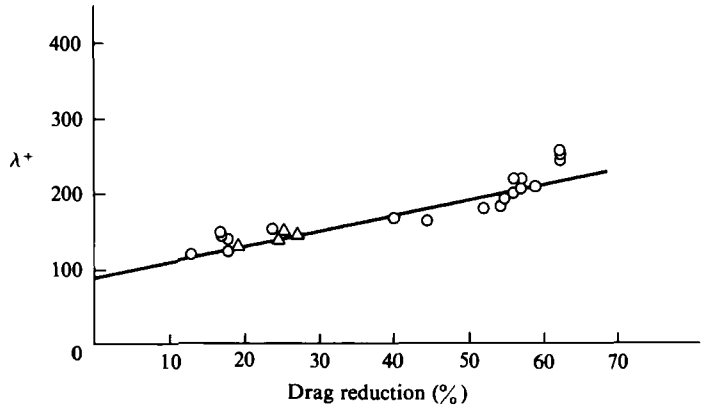

FIGURE 12. Effect of drag reduction of the dimensionless spacing of sublayer streaks: ○, Oldaker & Tiederman (1977); △, present study; ——, $\lambda^+ = 2.01$ (% DR) + 90.4.

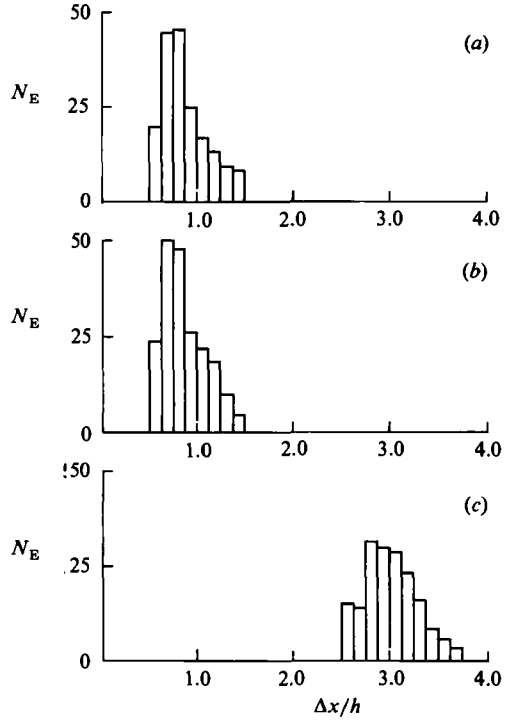

FIGURE 13. Ejection histograms for 1.30 mm slot; (*a*) water, $\Delta t = 4.17$ s; (*b*) 16 % glycerin, $\Delta t = 4.17$ s; (*c*) 100 p.p.m. AP-273, $\Delta t = 12.5$ s.

In figure 12, the dimensionless streak spacing for the experiments with drag reduction at the measurement location are compared with the drag-reduction results for fully mixed solutions of Oldaker & Tiederman (1977). The spacings measured in the present injection study as well as the spacings from the fully mixed experiments correlate with percentage drag reduction.

Ejection histograms for a water, 16 % glycerin and 100 p.p.m. polymer solution are shown in figure 13. In this figure $\Delta x/h$ was the distance downstream from the

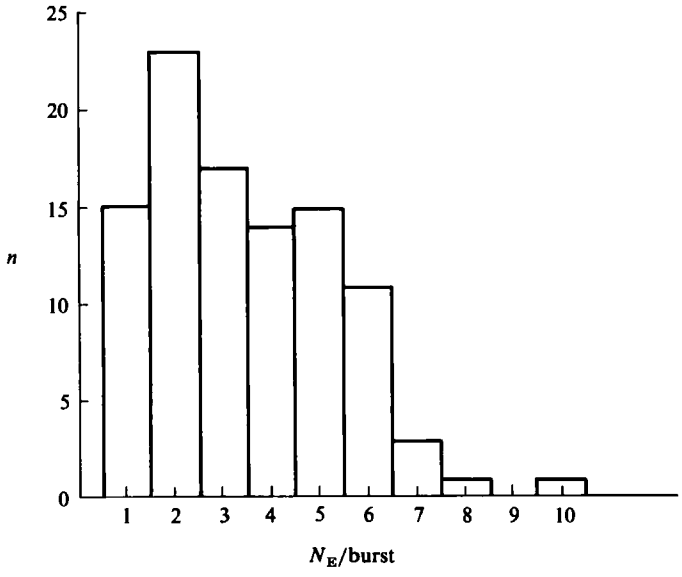

FIGURE 14. Histogram of the number of ejections per burst for a flow with 27 % drag reduction, $Re = 22300$ and $v^* = 3.70$ cm/s.

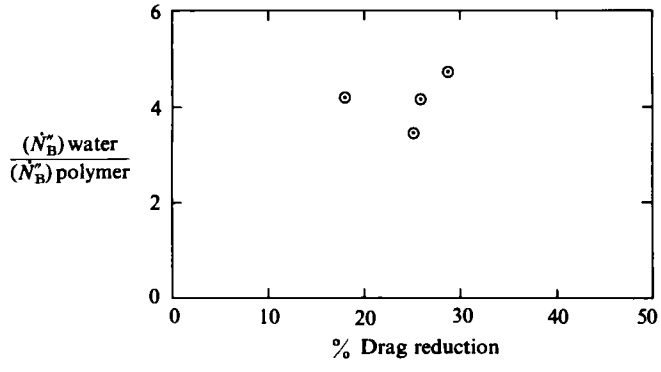

FIGURE 15. Comparison at equal values of wall shear velocity of the bursting rate per unit area for flows of water and flows with injection of drag-reducing polymer solutions.

flow-visualization slots and the time over which the ejections were counted was 3 times longer for the polymer injection than for the Newtonian fluids. Although the viscosity was different for the water injection and the 16 % glycerin injection, the frequencies of ejections in the full-detection region were quite similar. However, when the 100 p.p.m. polymer solution was introduced not only did the frequency of ejections decrease but the locations where all ejections were marked also moved downstream substantially. These changes indicate that the bursting rate in the near-wall region is altered greatly by the presence of the polymer.

To convert ejection rates to bursting rates it is necessary to know how many ejections occur per burst for the drag-reducing flow. (Recall that Newtonian flows have approximately two ejections per burst.) Using simultaneous top and side views of one streak and its related bursts, the number of ejections per burst was determined for a drag-reducing flow. The results are plotted in figure 14. Although the modal

value of the histogram is two, the average is 3.45. Thus, on average, approximately 3.45 ejections occurred per burst in this drag-reducing flow. Since all of the drag-reducing flows had approximately 25 % drag reduction in the streamwise region where ejection rates were measured it was assumed that the ratio of 3.45 ejections per burst was valid for each case.

Figure 15 shows the bursting-rate results for the drag-reducing flows. Although the data exhibits some scatter, it is clear that the bursting rate for the drag-reducing flow is much lower than that for a water flow at the corresponding shear velocity. Some of the bursting-rate values for the equivalent water flows were interpolated from the experiments shown in table 1 which span the range of shear velocities measured in the drag-reducing cases. This decrease in bursting rate is larger than the increase in streak spacing that occurs for drag-reducing flows. Consequently the results are in qualitative agreement with the data of McComb & Rabie (1982) and differ substantially from those reported by Achia & Thompson (1977), Donohue *et al.* (1972) and Tiederman *et al.* (1977).

4. Conclusions

The pressure-drop and flow-visualization results from the 0.130 mm slot experiments demonstrate that a thin region of drag-reducing polymer solution within *only* the linear, viscous sublayer does not alter the bursting rate of the wall-layer structures, modify the spanwise spacing of the wall-layer streaks, or lower the viscous drag. The sole modification that occurs when only the sublayer contains the drag-reducing polymer solution is a decrease in the mixing and transport between $y^+ \leqslant 2$ and $y^+ \approx 10$–15. These results strongly suggest that the linear sublayer is a passive participant in the interaction of the inner and outer portions of a turbulent wall layer. The convective motions within the linear sublayer appear to be primarily a response to more energetic motions which occur further from the wall. Grass (1971) envisaged a similar passive role for the sublayer.

Drag reduction begins downstream of the location where the injected, drag-reducing fluid has been ejected in turbulent bursts from the near-wall region. Flow visualization in the initial region of drag reduction downstream of the inclined slots shows that the dimensionless spanwise spacing of the wall-layer streaks has increased and the the bursting rate has decreased. This wall-layer structure has the characteristics of the wall-layer structure in a drag-reducing flow of well mixed, homogeneous polymer solution even though the injected polymer solution was not mixed uniformly with the main flow. Thus the drag-reducing additives appear to have a direct effect on the flow structures in the buffer layer, $10 < y^+ < 100$. The upper bound cannot be established precisely from this study. However, injection studies conducted with more concentrated solutions in turbulent pipe flows by McComb & Rabie (1982) yielded similar bursting-rate results as well as the value of $y^+ = 100$ as the upper bound of the effective region for the polymer additives.

This research was supported by the Naval Sea Systems Command General Hydromechanics Research (GHR) Program Subproject SR 023 01 01, administered by the David W. Taylor Naval Ship Research Development Center under office of Naval Research Contract number N 00014-81-K-0210 and by the Office of Naval Research, Contract number N 00014-83-K-0183, NR 062-754.

REFERENCES

ACHIA, B. U. & THOMPSON, D. W. 1977 Structure of the turbulent boundary layer in drag-reducing pipe flow. *J. Fluid Mech.* **81**, 439.

BOGARD, D. G. & TIEDERMAN, W. G. 1983 Investigation of flow visualization techniques for detecting turbulent bursts. In *Symposium on Turbulence, 1981* (ed. G. K. Patterson & J. L. Zakin), p. 289. University of Missouri-Rolla.

CANTWELL, B. J. 1981 Organized motion in turbulent flow. *Ann. Rev. Fluid Mech.* **13**, 457.

DONOHUE, G. L., TIEDERMAN, W. G. & REISCHMAN, M. M. 1972 Flow visualization of the near-wall region in a drag-reducing channel flow. *J. Fluid Mech.* **56**, 559.

ECKELMAN, L. D., FORTUNA, G. & HANRATTY, T. J. 1972 Drag reduction and the wavelength of flow-oriented wall eddies. *Nature, Lond.* **236**, 94.

GRASS, A. J. 1971 Structural features of turbulent flow over smooth and rough boundaries. *J. Fluid Mech.* **50**, 233.

KIM, H. T., KLINE, S. J. & REYNOLDS, W. C. 1971 The production of turbulence near a smooth wall in a turbulent boundary layer. *J. Fluid Mech.* **50**, 133.

KLINE, S. J., REYNOLDS, W. C., SCHRAUB, F. A. & RUNSTADLER, P. W. 1967 The structure of turbulent boundary layers. *J. Fluid Mech.* **30**, 741.

LUCHIK, T. S. & TIEDERMAN, W. G. 1984 Bursting rates in channel flows and drag-reducing channel flows. In *Symposium on Turbulence, 1983* (ed. X. B. Reed, G. K. Patterson & J. L. Zakin), p. 15. University of Missouri-Rolla.

MCCOMB, W. D. & RABIE, L. H. 1979 Development of local turbulent drag reduction due to nonuniform polymer concentration. *Phys. Fluids* **22**, 1983.

MCCOMB, W. D. & RABIE, L. H. 1982 Local drag reduction due to injection of polymer solutions into turbulent flow in a pipe. Part I: Dependence on local polymer concentration; Part II: Laser-Doppler measurements of turbulent structure. *AIChE J.* **28**, 547.

OFFEN, G. R. & KLINE, S. J. 1975 A comparison and analysis of detection methods for the measurement of production in a boundary layer. In *Proc. 3rd Biennial Symp. on Turbulence in Liquids* (ed. G. K. Patterson & J. L. Zakin), p. 289. University of Missouri-Rolla.

OLDAKER, D. K. & TIEDERMAN, W. G. 1977 Spatial structure of the viscous sublayer in drag-reducing channel flows. *Phys. Fluids* **20**, S133.

SMITH, C. R. & METZLER, S. P. 1983 The characteristics of low-speed streaks in the near-wall region of a turbulent boundary layer. *J. Fluid Mech.* **129**, 27.

TIEDERMAN, W. G., SMITH, A. J. & OLDAKER, D. K. 1977 Structure of the viscous sublayer in drag-reducing channel flows. *Turbulence in Liquids 1975* (ed. J. L. Zakin & G. K. Patterson), p. 312. Princeton: Science Press.

WELLS, C. S. & SPANGLER, J. G. 1967 Injection of a drag-reducing fluid into turbulent pipe flow of Newtonian fluid. *Phys. Fluids.* **10**, 1890.

WILLMARTH, W. W. 1975 Structure of turbulence in boundary layers. *Advances in Applied Mechanics*, vol. 15, p. 159. Academic.

WU, J. & TULIN, M. P. 1972 Drag reduction by ejecting additive solutions into pure-water boundary layer. *Trans ASME* D: *Basic Engng* **94**, 749.